Biomimetic Multiscale Hierarchical Topography Enhances Osteogenic Differentiation of Human Mesenchymal Stem Cells

Yang Liangliang; Ge Lu; Zhou Qihui; Mokabber, Taraneh; Pei Yutao; Bron, Reinier; van Rijn, Patrick

Published in:
Advanced Materials Interfaces

DOI:
10.1002/admi.202000385

ADVANCED MATERIALS INTERFACES
www.advmatinterfaces.de

Biomimetic Multiscale Hierarchical Topography Enhances Osteogenic Differentiation of Human Mesenchymal Stem Cells

*Liangliang Yang, Lu Ge, Qihui Zhou, Taraneh Mokabber, Yutao Pei, Reinier Bron, and Patrick van Rijn**

The interface between materials and cells plays a critical role in many biomedical applications. Inspired by the hierarchical architecture of collagen, most abundant structure in the extracellular matrix (ECM), a multiscale hierarchical topography is designed to mimic the collagen nano/micro hierarchical topography. It is hypothesized that the ECM topography affects osteogenesis of human mesenchymal stem cells but until now, it cannot be studied without the biochemical and mechanical influences of the ECM. The multiscale hierarchical topography is achieved by innovatively using sequentially aligned topography preparation via a silicone stretch-oxidation-release method and imprinting lithography. The anisotropically hierarchical topography influences stem cell morphology, orientation, and osteogenic differentiation. Intriguingly, the design resembling that of assembled collagen, exhibits the highest degree of osteogenesis. The hierarchical topotaxis effects are further exemplified by the enhanced vinculin expression, cell contractility, and more pronounced nuclear translocation of Yes-associated protein with the collagen-mimicking topography, indicative for enhanced osteogenesis. The developed multiscale hierarchical system provides insights into the importance of specific biological ECM-like topography by decoupling the biochemical influence. Various diseases, cancer, osteoarthritis, and fibrosis display impaired ECM structures, and therefore this system may have a great potential for tissue engineering approaches and developing in vitro disease models.

1. Introduction

There is a growing need for bioactive materials that are able to direct or enhance cellular behavior, including stem cell differentiation.[1–3] The development of artificial microenvironments that achieve control of stem cell fate is critical for effective stem cell therapies.[4] Proliferation, migration, and differentiation of stem cells are regulated by (bio)chemical signals (e.g., surface chemistry,[5] proteins[6]), biophysical cues (e.g., stiffness,[7,8] and geometry[9,10]), and cell–cell interactions.[11,12] Among the numerous environmental cues, the extracellular matrix (ECM) to which cells adhere, contains both biochemical, mechanical, and topographical cues and is still considered as the golden standard for creating an optimal material–cell interface.[13–16] A growing number of studies have highlighted the important role of substrate topography on the cell fate of different stem cell types,[17,18] and this can be modulated by the size and shape of surface topographical structures.[19–23] Aligned topographical features have been considered as a mimic of fiber-like ECM structures and have been used together with stem cells.[9,24,25] Previously, we identified the importance of both the height and pitch of the aligned surface structures on cellular behavior including variations in mechanical stimuli as well as providing double directional cues using metallic nanowire overlays to influence and guide cell morphology.[26–29] These systems provided much insight into the topography-guided cell response, but did not contain the topo-complexity that is found in the natural ECM.

L. Yang, L. Ge, R. Bron, Dr. P. van Rijn
Department of Biomedical Engineering-FB40 Groningen
University Medical Center Groningen
University of Groningen
A. Deusinglaan 1, Groningen 9713 AV, The Netherlands
E-mail: p.van.rijn@umcg.nl

The ORCID identification number(s) for the author(s) of this article can be found under https://doi.org/10.1002/admi.202000385.

DOI: 10.1002/admi.202000385

Dr. Q. Zhou
Department of Stomatology
Institute for Translational Medicine
The Affiliated Hospital of Qingdao University
Qingdao University
Qingdao 266003, China

T. Mokabber, Prof. Y. Pei
Faculty of Science and Engineering
Department of Advanced Production Engineering
Engineering and Technology Institute Groningen
University of Groningen
Nijenborgh 4, Groningen 9747 AG, The Netherlands

The ECM has inspired biointerface research and a deeper understanding of the biochemical interplay between ECM and cells contributed strongly to the field of biomedicine.[30,31] However, it is challenging to mimic the topographical features of the ECM, which are multiscale hierarchical micro/nano-structures and the focus is most often on recreating the biochemical or mechanical microenvironment.[32,33] Although, the ECM is often considered as a random fiber-mesh material, there are highly oriented natural ECM structures found in various tissues, including bone, nerve, and muscle.[34–37] In addition to the meso-scale aligned fibers in various tissues, ECM components such as collagen, also consist of a complex hierarchical nano/micro structure.[38] Bone consists for 30% of collagen. Collagen protein molecules formed from three chains of amino acids are a few nanometers in size, and individual collagen fibrils tend to be approximately hundreds of nanometers, whereas actual collagen fibers formed by multiple fibrils are tens of micrometers.[38] More importantly, wavy wrinkle-like structures could be clearly distinguished on the single collagen fiber, and their direction is perpendicular to collagen fiber (**Figure 1**A).[39] To date, cells can sense and interact with the smallest feature size of a substrate at approximately 5 nm.[40] Therefore, the hierarchically topographical cues containing micro- and nano-features may be regarded as essential for regulating stem cell fate, which may be a critical factor to consider for the design of synthetic ECMs.[41] Notably, the differently sized features affect the cellular behavior in a specific fashion. Micro- and nano-sized topographies influence cells by changing cellular morphologies along with the patterns giving rise to the re-organization of the actin cytoskeleton[42] and activating the integrin-mediated intracellular signaling cascade,[43] respectively, thus modulating stem cell differentiation in a synergistic way. Chung and co-workers[41] developed hierarchically micro- and nanopatterned transplantable patches to study the adhesion and differentiation of human mesenchymal stem cells (hMSCs). However, they only investigated the parallel combination for nano/micro-sized structure, which does not mimic the hierarchical architecture of collagen.

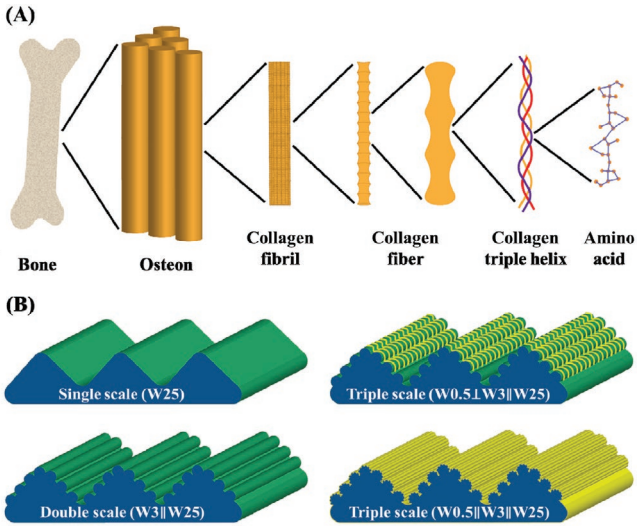

Figure 1. A) Hierarchical architecture of collagen in natural bone. Osteons comprise mineralized collagen fibrils, composed of single collagen fiber and collagen protein molecules (tropocollagen) formed from three chains of amino acids. B) Biomimic the hierarchical structures of collagen with synthetic material (PDMS) in vitro (single, double, and triple scale substrates), and this enables us to deactivate the biochemical factor easily and solely focus on the influence of topography on stem cell behavior.

Herein, we hypothesize that the highly defined multiscale hierarchical structure of collagen in vivo modulates the morphology and influences osteogenic differentiation of human Bone Marrow-derived Mesenchymal Stem Cells (hBM-MSCs). With the use of collagen, it is not possible to deactivate the biochemical component easily and solely focus on topography. Additionally, it is not possible to vary the nanotopographical features of collagen while maintaining the integrity of the fiber structures. Therefore, to test this hypothesis, we developed substrates with well-defined hierarchical multiscale topographies through a silicone stretch-oxidation-release method and imprinting lithography. Based on this approach, single scale (Flat, W0.5, W3, and W25), double, and triple scale (W0.5, W3, and W25 combined with different direction [parallel, perpendicular, 45°]) were prepared (Figure 1B). The sizes chosen are independently well distinguishable and the orientation could be controlled to an excellent degree. Although the feature sizes do not exactly match the sizes found in collagen, they are in the same order and the hierarchical build-up and orientation is mimicked very well with the important possibility to vary the relative orientation in order to test the hypothesis that the found hierarchy in collagen is important for cells to respond to. Using these platforms, we investigated the influence of anisotropically hierarchical wrinkle structure on the morphology, orientation, and osteogenesis of hBM-MSCs. Furthermore, we examined the connection between osteogenesis and expression of vinculin, cell tension, and Yes-associated protein (YAP)-TAZ pathway to illustrate the mechanism underneath. It is the first time that the hierarchically multiscale structures which better mimic the collagen architecture in ECM of bone are used to explore stem cell differentiation in vitro.

2. Results

2.1. Hierarchical Structured Substrate Preparation and Characterization

The ECM of bone has an anisotropic architecture consisting of well-aligned nano/micro-scale structures. However, it is important to highlight that the surface of a collagen fiber is also structured with a wavy-like architecture rather than being smooth (Figure 1A). Thus, the developed system would provide a method to address the hypothesis that whether or not well defined hierarchically topography consisting of nano- and micropatterned structure as found in collagen bundles aid in the guidance of cells and direct the commitment of stem cells.

To mimic the hierarchical structure of collagen, the main ECM component of bone, a methodology to fabricate multiscale hierarchical PDMS substrates was first developed by a combination of sequentially aligned topography preparation via a silicone stretch-oxidation-release method and imprinting lithography. **Figure 2** shows the schematic approach of the fabrication of multiscale hierarchical substrates. After the fabrication of the single scale substrate (the conditions were summarized

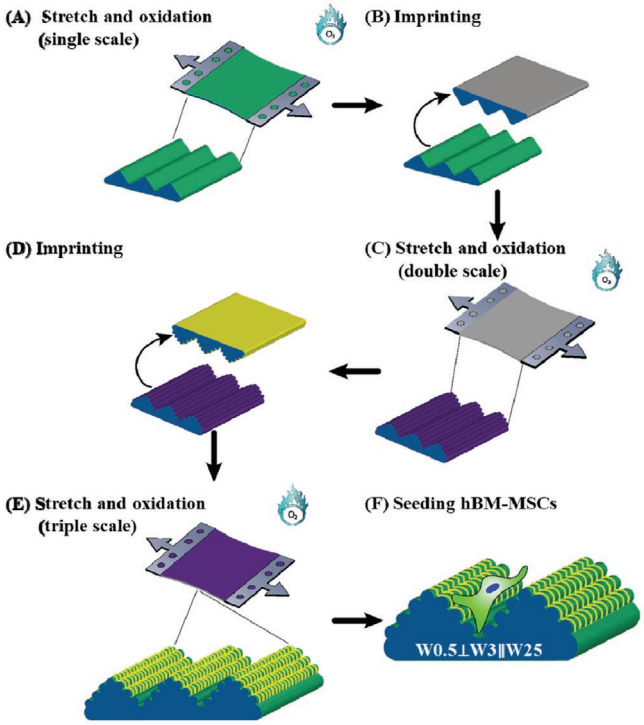

Figure 2. Schematic illustration of the fabrication of various scales wrinkle substrates. A) After PDMS membrane stretched and oxidized, uniform single scale wrinkle emerged. B,D) Imprinting process to obtain a newly soft substrate with the same topography of mold. C,E) Stretch and oxidize the new substrate again to prepare the double and triple scale substrate, respectively. F) hBM-MSCs were seeded onto the triple scale hierarchical substrate.

in Table S1, Supporting Information), the multiscale hierarchical topography was prepared in a sequential fashion of a repeating procedure. This procedure provides control of the orientation of the newly added topography with respect to the previous topography by controlling the stretching direction. It is worth noting that the addition of a new topography was done by adding a smaller feature on top of the larger feature rather than the reverse. In addition, the surface of the substrate will form a glass-like (SiO_2) layer after the oxidation process, so it is critical that an imprint of the topography in pristine PDMS is prepared before the preparation of double and triple scale topography substrates. This substrate can then be stretched and oxidized for implementing the next topography. It provides the possibility to create the hierarchical structure in a highly controlled fashion with impeccable control of the orientation of the aligned topographies with respect to one another. In this study, three different scaled hierarchical topography substrates were prepared: triple scale (0.5∥3∥25, 0.5⊥3∥25, and 0.5⊥3∠25), double scale (parallel: 0.5∥3 and 0.5∥25; perpendicular: 0.5⊥3 and 0.5⊥25; and 45°combination: 0.5∠3 and 0.5∠25), and single scale (Flat, W0.5, W3, and W25). It has to be noted that in order to keep the same surface and mechanical properties, all single scale and multiscale substrates were implemented the same imprinting process (10:1 for elastomer base and cross-linker) and oxidization condition (500 mTorr for 1 min) for further cell experiments.

The surface features after imprinting were characterized by atomic force microscopy (AFM). As shown in Figure S1, Supporting Information, wave-like topographies (single scale) were achieved with varying dimensions (wavelength [*W*; μm] and amplitude [*A*; μm]) of W0.5A0.05, W3A0.7, and W25A4.3. The different surface topographies are further reported as Flat, W0.5, W3, and W25. The angle between the different topographies was varied by controlling the stretching direction of the freshly imprinted structures. Although any angle (orientation) may be chosen, we limited the system here to 0° (parallel), 45° (oblique), and 90° (orthogonal). As shown in **Figure 3**, W0.5 and W3 topography were formed onto the surface with the W25 topography by following the described procedure (lower magnification of images are shown in Figure S2, Supporting Information). The height profiles of wrinkle structure were displayed below the AFM images.

Importantly, for triple scale substrates, W0.5 and W3 could be clearly observed on the top of W25 with different combinations of the topography directions. Besides, the surface of triple scale hierarchical substrates was characterized by environmental scanning electron microscopy as displayed in **Figure 4**, and the lower magnification images are shown in Figure S3, Supporting Information, also displaying the morphologies of the hierarchical structures. Taken together, the results demonstrate that our innovative fabrication method is scalable and tunable, providing complex multiscale hierarchical topography substrates that mimic the structure build-up of collagen. Therefore, this enables us to investigate the influence of multiscale architecture on stem cell behavior.

2.2. Morphology and Orientation of hBM-MSCs Affected by Multiscale Topography

Cell elongation and orientation are the morphological features essential for many anisotropic tissue functions.[44] Using the micro- and nanosized hierarchical structure as cell culture substrates, we explored the effect of hierarchical topography on the morphology and orientation of hBM-MSCs. To this end, we fabricated three scales of micro- and nanopatterned hierarchical substrates as well as a Flat surface as a control. Cells were cultured for one day on substrates with topography composed of different levels of hierarchy (single, double, and triple scale). Cell alignment, expressed as the percentage of cells that have their main axis within 10° from the direction of the topography,[45,46] was quantified with Fiji software. As shown in **Figure 5**, cell morphology and orientation were strongly influenced by the multiscale hierarchical structure.

From immunofluorescent imaging and quantification of results for cell orientation, it was seen that hBM-MSCs grown on Flat and W0.5 showed isotropic fibrous F-actin networks (phalloidin staining of the cytoskeleton) and were randomly oriented (the orientation degree was 17% for W0.5). In contrast, W3 and W25 substrates promoted orientation of cells along the long axis of the topography, and cell orientation was 59% and 58%, respectively. This illustrates that larger topographies (W3 and W25) resulted in cells with highly elongated shapes compared to Flat substrates, which coincides with our previous results.[28,47] For the double scale substrates, hBM-MSCs

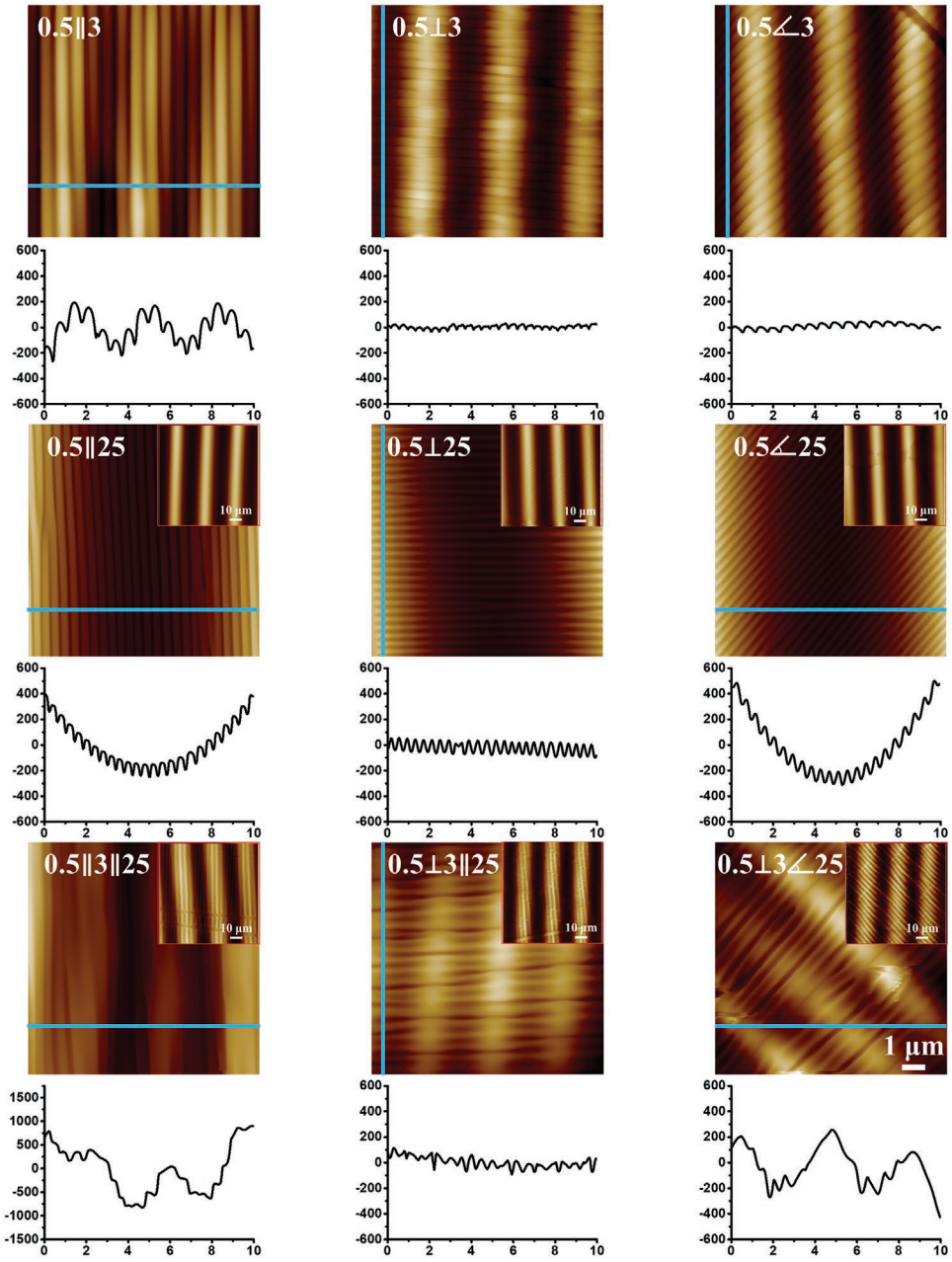

Figure 3. AFM images and height profiles of the structured PDMS surfaces obtained after imprinting. The colored lines stand for the position from AFM image to draw the height profiles ($n \geq 30$ wrinkles for each imprint, three independent imprints). Scale bar is 1 µm. Inset shows the image with a lower magnification (showed in Figure S2, Supporting Information) and the scale bar is 10 µm.

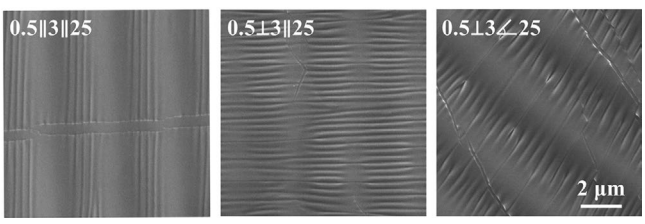

Figure 4. Representative SEM images of the triple scale substrates. Scale bar is 2 µm.

on parallel direction (0.5||3 and 0.5||25) showed more aligned F-actin fiber bundles and the cells were more elongated and orientated along the direction of wrinkles (80% and 60%, respectively). In contrast, cells on the substrates with perpendicular direction (0.5⊥3, 0.5⊥25) showed less degree of elongation and orientation (71% and 51%, respectively). Interestingly, cells on 0.5||3 and 0.5||25 showed more alignment and orientation compared to those on single scale substrates (W0.5, W3, and W25). The triple scale substrate, 0.5||3||25, induced the strongest cell elongation and the highest degree of orientation (96%), much

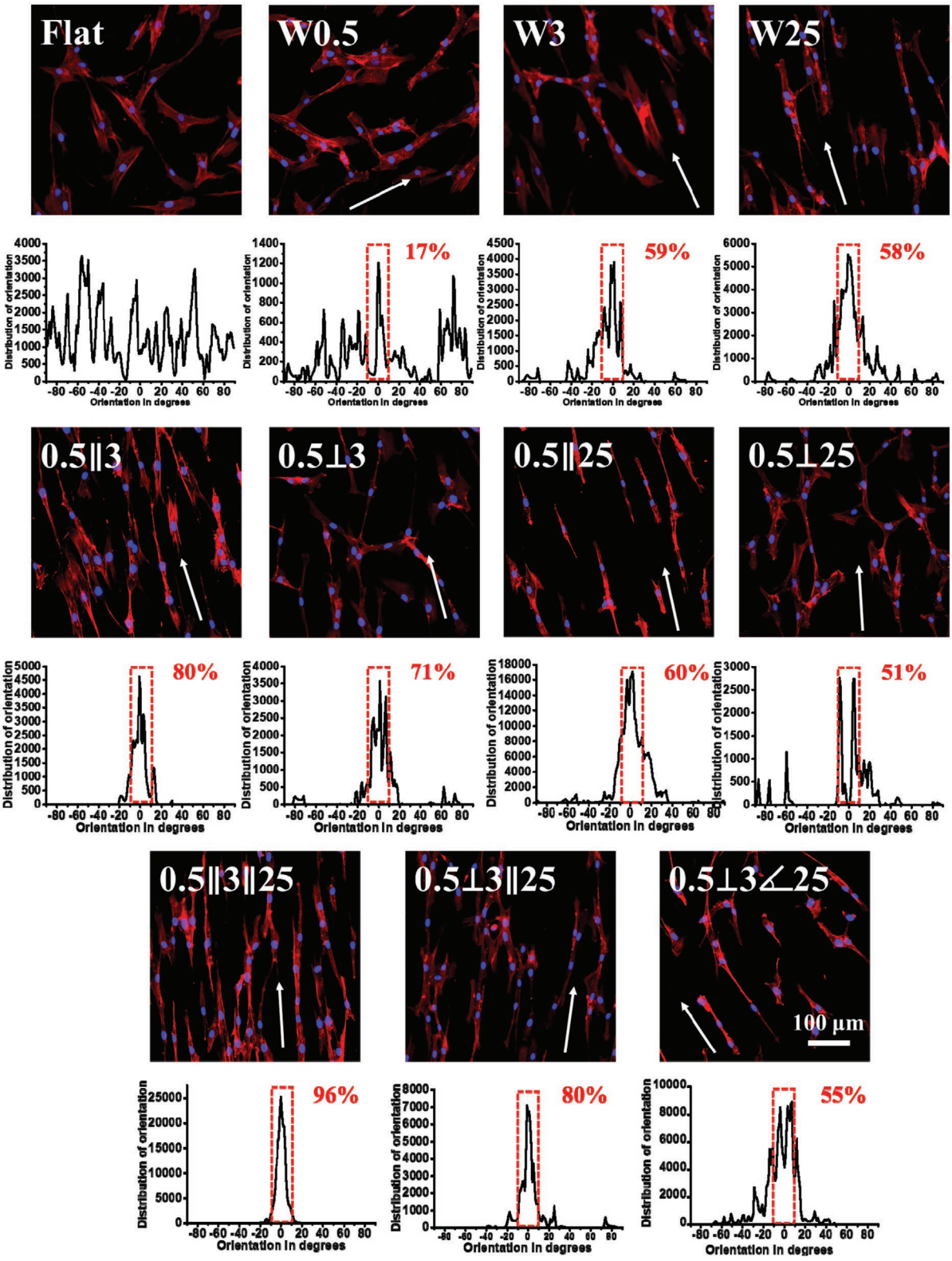

Figure 5. Influence of multiscale hierarchical structure on the morphology and orientation of hBM-MSCs. The upper row was the representative immunofluorescent images of hBM-MSCs grown on different topographies, and the lower row stand for the distribution of cell orientation with respect to the direction of the applied topography. Cell cytoskeleton and cell nucleus were stained with TRITC-labeled phalloidin (red) and DAPI (blue), respectively. The white arrow indicates the direction of wrinkle with the larger wavelength. Totally ≥8 images per sample and 3 independent samples were analyzed. The scale bar for all the images is 100 μm.

higher than the other two triple scale substrates (80% for 0.5⊥3‖25 and 55% for 0.5⊥3∠25) and the single and double substrates. This difference indicates that cell morphology was greatly dependent on the combined direction of multiscale substrate and specific parameters. In addition, we also quantified the cell area (two dimensions) by actin staining after cultured for one day (Figure S4, Supporting Information). Compared to single scale substrates (except W25), cell area for double and triple scale substrates significantly decreased. The cells cultured on the group of 0.5⊥3∠25 substrate had the smallest cell area (about 900 μm^2), much smaller than that on the double scale substrates (around 1250 μm^2). Collectively, our finding suggest that hierarchical structures consisting of nano/micro-size and the direction between the different combinations of topography have a synergistic role in adjusting the macroscopic behavior of hBM-MSCs.

2.3. Enhancement of Osteogenesis of hBM-MSCs by the Hierarchical Structure

Because collagen with its hierarchical topography is abundant in bone, we next assessed the effect of micro- and nano-structured hierarchical topography on the osteogenesis of hBM-MSCs. To this end, we cultured stem cells on the substrates in osteogenic induction medium (OM) for 14 and 21 days. The degree of osteogenesis of hBM-MSCs was determined by quantitative alkaline phosphatase (ALP) and osteopontin (OPN) immunofluorescent staining which was assessed via automated imaging (TissueFaxs). The automated approach enables that imaging is done using the same parameters for the whole imaging process. The final functional differentiation state, namely the formation of mineral, was further confirmed by Alizarin Red staining. The Flat surface was used as a control group.

2.3.1. ALP and OPN Expression

ALP is an important early marker for the osteogenic differentiation of stem cells.[48] Therefore, the detection of ALP activity is essential to evaluate the osteogenic differentiation degree of hBM-MSCs.[49] **Figure 6**A shows hBM-MSCs cultured in OM for 14 days and various fluorescence density of stained ALP was observed among single, double, and triple scaled hierarchical substrates.

For the single scale substrate, there was enhanced expression of ALP on W3 compared to W0.5 and W25, however, cells showed minimal expression of ALP on Flat substrate (Figure S5, Supporting Information). Interestingly, for the double scale surface (Figure 6A), cells cultured on 0.5⊥3 and 0.5⊥25 had stronger ALP intensity compared to 0.5‖3 and 0.5‖25, respectively, suggesting that the direction of multiscale substrate had an important influence on ALP expression. For the triple scale substrates, ALP activity of hBM-MSCs grown on 0.5⊥3‖25 was significantly improved compared to the cells on 0.5‖3‖25 and 0.5⊥3∠25, indicating that the structure which resembles the collagen topography promotes osteogenic differentiation of hBM-MSCs. These effects were quantified by assessing the fluorescence intensity for the 14 days differentiation and the results were shown in Figure 6C. The fluorescence output was normalized for the cell number and it correlated well with the qualitative analysis. The results showed that 0.5⊥3 and 0.5⊥25 significantly facilitate osteogenic differentiation of hBM-MSCs as illustrated by a 2.3- and 3.2-fold increase, respectively, as compared to the Flat substrate. The difference became even more striking among triple scale hierarchical substrates, where a 5.5-fold increase was observed for 0.5⊥3‖25. Except for ALP, we also examined the OPN, as it is a late marker in the differentiation process.[50] The results (Figure 6B,D) follow a similar trend as for ALP. For the double scale substrates, the expression of OPN, as indicated by the presence of fluorescence signal, was higher in cells cultured on 0.5⊥3 and 0.5⊥25 than those on the 0.5‖3 and 0.5‖3, respectively. For the triple scale substrates, the intensity was the highest in cells cultured on 0.5⊥3‖25 compared to other two substrates (0.5‖3‖25 and 0.5⊥3∠25). Taken together, these results indicate the importance of the specific biological hierarchical arrangement of collagen on cell differentiation.

2.3.2. Mineralization Affected by the Specific Orientations of the Hierarchical Topographies

The generation of mineralized nodules, caused by the calcium secretion of MSCs, is a vital function indicator of osteoblasts that is usually used to evaluate the osteogenic differentiation of MSCs[51] and can be confirmed by Alizarin Red staining.[52] To assess the degree of osteogenesis, hBM-MSCs cultures were stained using Alizarin Red after 21 days of culturing in OM. From the results of ALP and OPN expression for 14 days, the triple scaled hierarchical substrates were selected. The images of Alizarin Red staining showed substantial differences between the different substrates (**Figure 7**A). The results demonstrate that the calcium expression was higher for hBM-MSCs cultured on the 0.5⊥3‖25 substrate than on the other two substrates (0.5‖3‖25 and 0.5⊥3∠25) and this was in line with the highest expression of both ALP and OPN. To quantify the degree of osteogenesis of hBM-MSC, the stained calcium deposits were de-stained, and the optical density (OD) of the extracted mineral phase was measured. As shown in Figure 7B, the highest OD_{540} was obtained for cells grown on 0.5⊥3‖25 followed by those on 0.5⊥3∠25, and the lowest for 0.5‖3‖25. This further confirms that 0.5⊥3‖25 substrates enhanced osteogenic differentiation, while culturing on 0.5‖3‖25 suppressed osteogenesis. Overall, these results further indicate that the spatial distribution of surface topographies as well as topography shapes and dimensions are critical for the differentiation of stem cells. Therefore, it suggests that hierarchically multiscale topographies are extremely important in the structure of collagen and that it is not just a mere presentation of biochemical factors such as the cell-binding sites present within the collagen amino-acid sequence.

2.4. Focal Adhesion, Cell Tension, and YAP-TAZ Signal Pathway Affected by the Hierarchical Structure

Based on the significant difference among triple scale substrates for osteogenic differentiation, attention was paid to the formation of focal adhesions (FA), the direct communication tool of

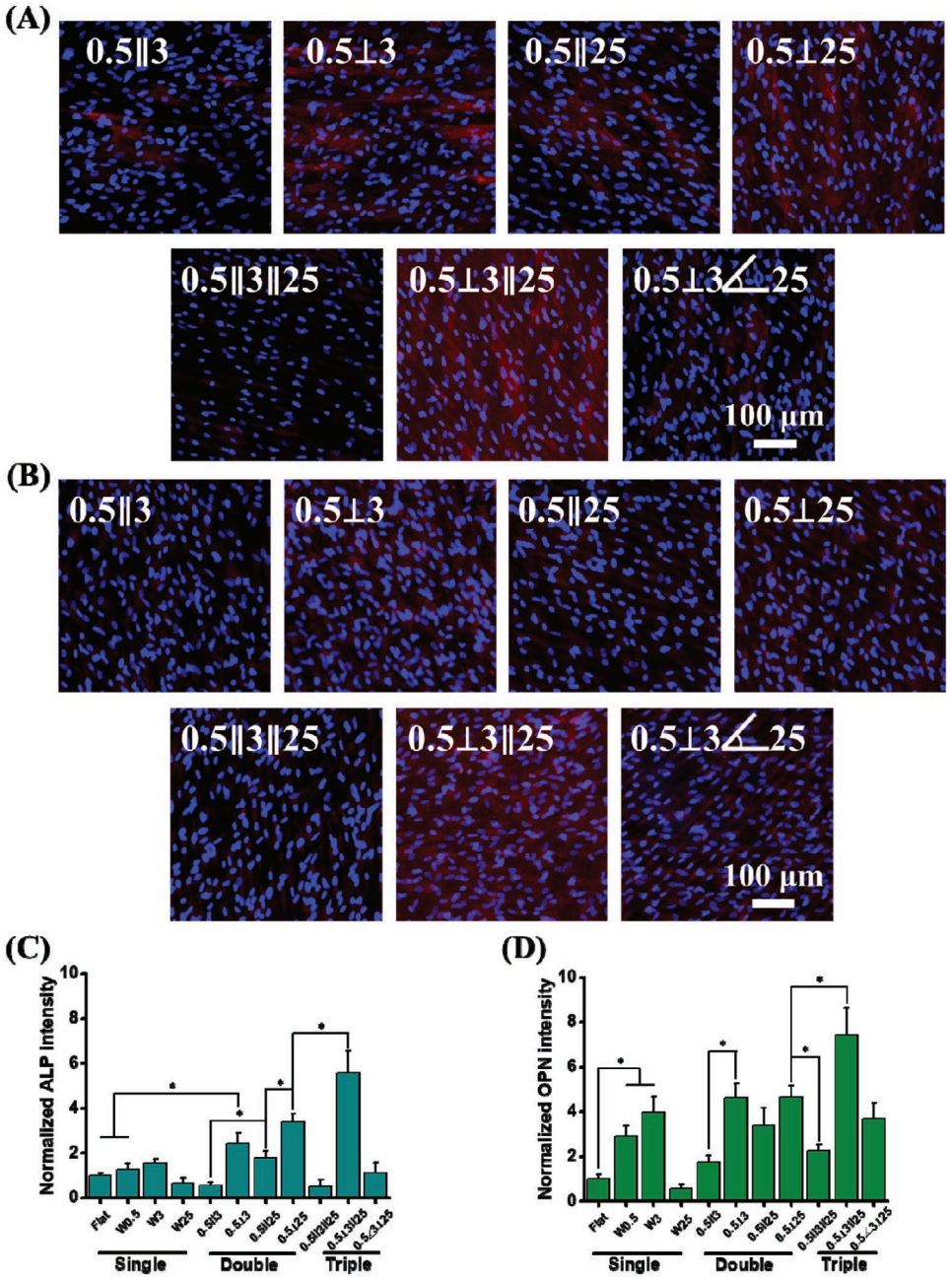

Figure 6. Immunofluorescence staining of osteogenic marker A) ALP and B) OPN of cells grown on double and triple scale substrates cultured in OM for 14 days. Cells were stained for DAPI (nucleus, blue), and ALP/OPN (red). The scale bar for all the images is 100 µm. Quantification of the expression of C) ALP and D) OPN in cells cultured in OM at day 14, normalized by cell number ($n \geq 100$ cells and each experiment was performed in triplicate). Data are shown as mean ± standard deviation (SD), and $^*p < 0.05$.

cells with their environment. FA are adhesion plaques formed by an assembling complex of integrins and proteins.[53] It has been demonstrated that the formation of FAs are related with the RhoA/ROCK signaling pathway by affecting the cytoskeleton and cell contractility and it was also found that more formation of FAs are beneficial for osteogenesis.[54,55] Our previous study has reported that topographical dimension can provide significant stimulation to influence the organization of focal adhesion complexes.[28] The expression of FAs in hBM-MSCs was assessed by immunofluorescence staining for vinculin and visualized by confocal laser scanning microscopy after 24 h seeded onto the different substrates. As shown in **Figure 8**A, significant differences in focal adhesion number and morphology were observed. For substrates of 0.5⊥3‖25 and 0.5⊥3∠25, hBM-MSCs had more well-defined dash-like vinculin spots (typical regarded as mature focal adhesions). In contrast, cells grown on 0.5‖3‖25 showed dot-like (transient) vinculin spots, indicating that 0.5⊥3‖25 and 0.5⊥3∠25 could enhance the expression of vinculin. To better

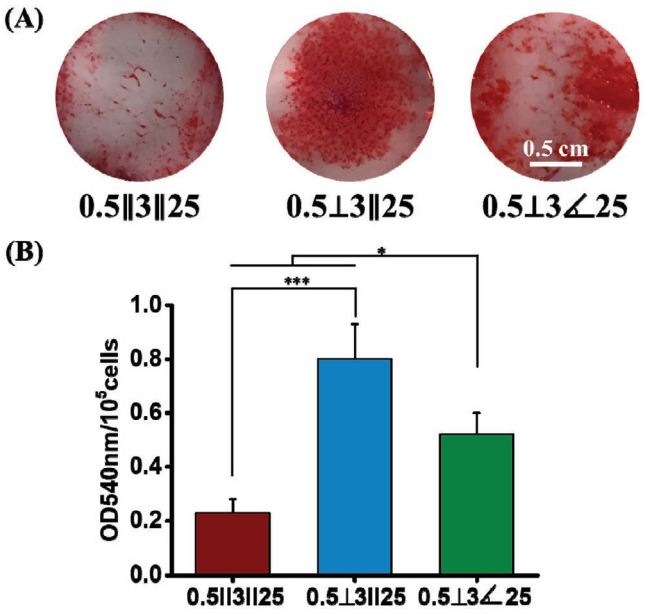

Figure 7. A) Representative images of calcium nodules stained with Alizarin Red showing extracellular calcium deposits by hBM-MSC-derived osteoblasts cultured in OM for 21 days. B) Mineralization quantitated by elution of Alizarin Red staining from stained mineral matrix. Data were shown as mean ± standard deviation (SD), each experiment was performed in triplicate, and $*p < 0.05$, $***p < 0.001$. Scale bar represents 0.5 cm.

understand the focal adhesion formation on different substrates, FA area per cell was quantitatively analyzed (Figure 8B). FA area for cells cultured on 0.5⊥3‖25 (294 μm^2) and 0.5⊥3∠25 (257 μm^2) are much higher than 0.5‖3‖25 (216 μm^2). These results indicate that comparing substrates with the same anisotropical hierarchical features, the relative direction of the features with respect to one another greatly influence the formation of FAs.

Cytoskeletal contractility and tension can be characterized by phosphorylated myosins.[15] A further study on cell tension was performed to speculate whether or not cell tension influences the lineage commitment of stem cells. In our study, immunofluorescent staining of myosin was performed for hBM-MSCs after 24 h cell culture. The immunostaining results (Figure 8C) showed that for cells grown on 0.5⊥3‖25 and 0.5⊥3∠25, stronger fluorescence intensity was observed compared to 0.5‖3‖25. The quantification (Figure 8D) was consistent with the observation from immunostaining images. It shows that myosin expression for cells grown on 0.5⊥3‖25 and 0.5⊥3∠25 was significantly enhanced about 4.3- and 3.3-fold higher than cells on 0.5‖3‖25, indicating that 0.5⊥3‖25 and 0.5⊥3∠25 substrates could improve the expression of myosin, illustrating a stronger cell contractility/tension. These results suggest that hierarchical structure greatly influences cell contractility.

Biophysical stimuli regulate the functionality of the transcription cofactors YAP and TAZ, which is a key regulatory element that controls the gene expression and is located either in the cytosol or in the nucleus as a consequence of the physical stimuli that the cells receive.[56] When in the nucleus, the paralogs YAP-TAZ modulate gene expression, but upon phosphorylation, they are sequestered in the cytoplasm.[57] The huge difference in the osteogenesis behavior on the triple scale structure urged us to investigate whether downstream signaling pathways are also affected, as YAP-TAZ signaling is known to be responsible for many downstream transcriptional outcomes of mechanotransduction.[58,59] Here, we examined its expression in the hBM-MSCs on different structures of triple scale hierarchical substrates. The expression of YAP-TAZ in hBM-MSCs was assessed by immunofluorescence staining 24 h after being seeded onto the different topographies. As shown in Figure 8F, the direction of hierarchical topography had a substantial effect on the localization of YAP-TAZ for which the percentage of YAP-TAZ located in the nucleus was quantified, which is a commonly adopted method to illustrate the topo-sensitivity.[60,61] The results showed that for cells cultured on 0.5⊥3‖25 and 0.5⊥3∠25 substrates, YAP-TAZ was present in the nucleus for about 66%, and 51% of the cells, respectively (Figure 8F). In contrast, expression of YAP-TAZ for cells cultured on 0.5‖3‖25 was predominantly cytoplasmic and the percentage of cells with positive nuclear YAP-TAZ was only 30%. Taken together, these results imply that the enhanced osteogenic differentiation of hBM-MSCs was partially mediated by YAP-TAZ signaling, cell contractility, and focal adhesions.

3. Discussion

Preparing an effective substrate platform that could better mimic the ECM structure in vivo and further manipulate cellular functions is very important for both understanding the importance of specific topographical cues in natural ECM components and promoting the development of stem cell-based therapy for clinical applications.[62,63] Previous studies demonstrated that the fate of stem cells are sensitively regulated by the stiffness and topography of substrates.[4,9,64–66] Regarding fabricating platforms that mimic the topographical features of ECMs, little attention has been devoted to the hierarchical property of ECMs due to technical limitations.[67,68] In other words, the current fabricated simple topographies cannot provide cells with the precisely defined biophysical cues of native physiological microenvironments composed of nano- and microscale topographies, which may cause a major barrier for constructing functional tissues or organs. To address this challenge, we developed a synthetic ECM-like structure fabrication approach with hierarchically micro- and nanopatterned surfaces with precisely controlled sizes and directions. Furthermore, the effects of hierarchical structure on cellular behavior and stem cell differentiation were investigated. Although, more closely mimicking the real size features would further enhance the topography mimicking approach of collagen, this study does illustrate the important role of hierarchical structures and their defined orientations in modulating the cell behavior and osteogenic differentiation.

It is generally known that hierarchical topography consisting of micro- and nanoscale structure adjusts stem cell differentiation via the synergistic modulation the elongation/orientation of cell cytoskeleton and intracellular focal adhesion protein assembly.[4,9] On the one hand, researchers have shown that for cell elongation the optimal cell aspect ratio for osteogenic differentiation is about 2, let alone with or without external chemical induction factors, indicating that cell shape itself is an inherent factor in regulating stem cell differentiation.[69] On the other hand, the anisotropic nanotopographies are known to

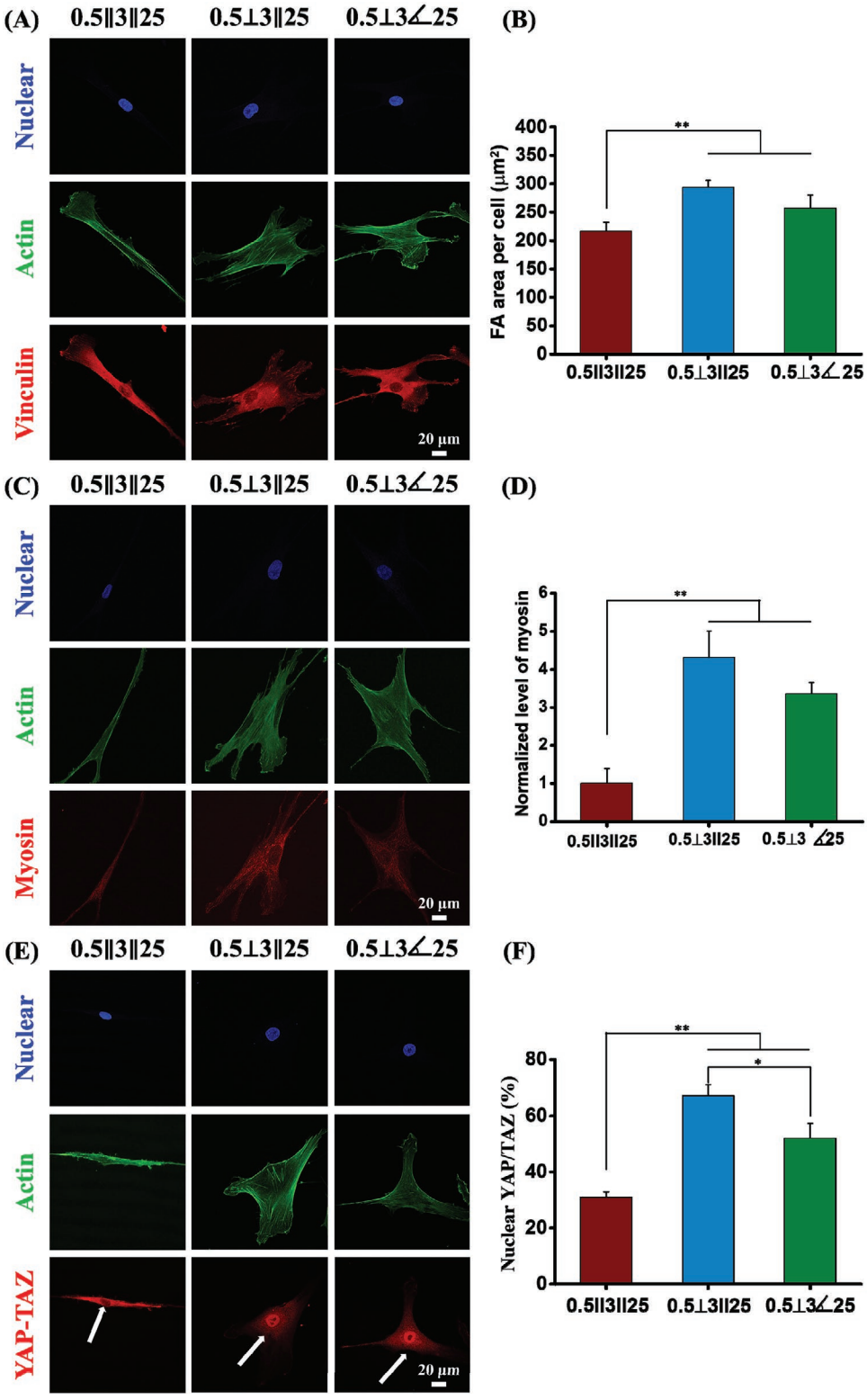

Figure 8. Immunofluorescent staining of nuclei (blue), A) vinculin/C) myosin/E) YAP-TAZ (red), and actin (green) for hBM-MSCs after 1 day cultivation on different substrates. The enlarged image for YAP-TAZ staining is included in Figure S6, Supporting Information. The white arrows refer to the location of interest for nuclear YAP-TAZ localization. Scale bar represents 20 μm. Quantitative analysis of B) FA area per cell, D) integrated fluorescence intensity of myosin, and F) the number of cells with nuclear localization of YAP-TAZ. Data are shown as mean ± standard deviation (SD), $n \geq 30$ cells (each experiment was performed in triplicate), and $^{*}p < 0.05$, $^{**}p < 0.01$.

enhance the osteogenic differentiation of stem cells via facilitating focal adhesion and actin polymerization.[1,70] Researchers demonstrated that a hierarchical substrate platform with microgroove (groove size: 1.5 μm) and nanopore (pore diameter: 10 nm) synergistically promoted neuron differentiation of neural stem cells, and the focal adhesion was increased on the hierarchical substrates because of the nanopore structures.[4] In addition, our previous study has reported that the width of aligned microtopographical patterns could force cell body to align and grow along the direction of wrinkle substrates because of space restriction, and the topographical dimension can provide significant stimulation to influence the organization of focal adhesion complexes.[28,47]

In our study, the reason for the highest degree of osteogenic differentiation for 0.5⊥3‖25 is probably due to microscale wrinkle structure providing the elongated and orientated cytoskeleton, and nanoscale cue that gives rise to the enhanced focal adhesion and actin organization via the RhoA/ROCK pathway. Compared to the other two triple scale substrates (0.5‖3‖25, 0.5⊥3∠25), cells cultured on 0.5⊥3‖25 have the highest degree of osteogenesis (Figures 6 and 7). Cells had the longest elongation for the substrate of 0.5‖3‖25 among three triple scale substrates, which exceed the optimal cell aspect ratio for improving osteogenesis. For 0.5⊥3‖25, cells exhibited larger focal adhesion area probably due to the nanometer structure (W0.5), further promoted cell tension/contractility and more YAP-TAZ (Figure 8) translocated into cell nucleus, giving rise to the enhanced osteogenic differentiation. We present a schematic mechanistic explanation that describes the substrate which biomimic structure of collagen induced an accelerating effect on the osteogenic differentiation (**Figure 9**).

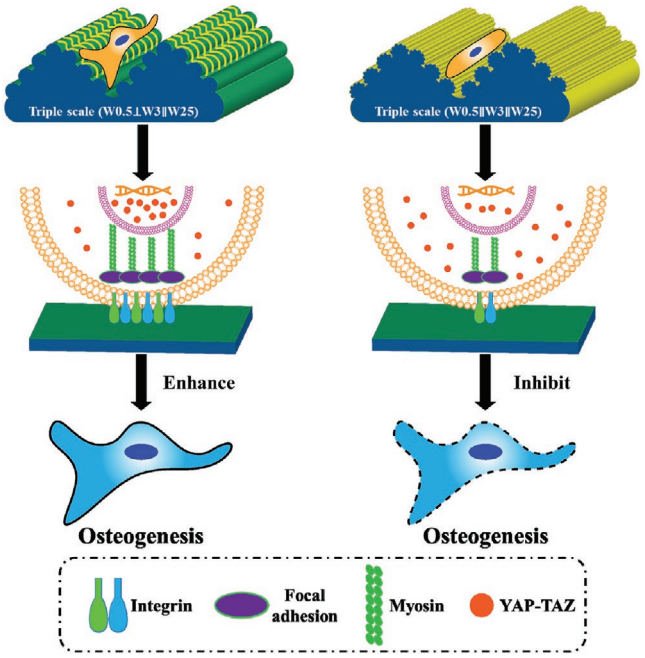

Figure 9. Schematic representation of the interaction between hBM-MSCs and hierarchical structure. 0.5⊥3‖25 substrate mimicking the hierarchical structure of collagen allows stem cells to have more focal adhesion, stronger intracellular tension, yielding more YAP/TAZ nuclear localization, and subsequently enhancing the osteogenic differentiation.

However, further investigations are necessary to fully elucidate the signal pathway involved in the regulation osteogenesis of hBM-MSCs stimulated by the hierarchical platform.

Our multiscale hierarchical substrates have other possible applications in the field of stem cell-based tissue engineering. For instance, precisely defined multiscale hierarchical topographies consisting of micro- and nano-size could further be used as a strategy for the design and fabrication of functional scaffolds. In this study, while focused on osteogenic differentiation for bone regeneration, we expect to mimic the native structure of hierarchical architecture of ECM in other tissues, such as nerve, tendon, and muscle, as these tissues also have hierarchical architectures at multiple scales, which size ranging from nanometer to hundreds of micrometers. Therefore, this multiscale hierarchical platform has great potential in facilitating application development for tissue engineering and regenerative medicine approaches.

4. Conclusion

For the first time, a multiscale hierarchical substrate is successfully designed and prepared to mimic the hierarchical architecture of collagen. An innovative approach was developed involving sequentially aligned topography preparation via a silicone stretch-oxidation-release method and imprinting lithography. It is found that the hierarchical topographies have a significant influence on the morphology, orientation, and osteogenic differentiation of hBM-MSCs. Intriguingly, the 0.5⊥3‖25 substrate, resembling collagen topography/structure the most, exhibits the highest capacity of osteogenesis. We further demonstrate that the differences in cell response among triple scale substrate is regulated via the focal adhesion, cell tension, and YAP-TAZ signaling pathway. Together, our work illustrates the significance of platforms that mimic the native structure of collagen, and provides insight into the design and manipulation of functional engineered constructs using multiscale hierarchical topography-based substrates for various biomedical applications, including stem cell therapy and tissue engineering.

Supporting Information

Supporting Information is available from the Wiley Online Library or from the author.

Acknowledgements

L.Y. and L.G. contributed equally to this work. The authors are very grateful for financial support of the China Scholarship Council (no. 201608310113 and 201707720058) and the UMCG Microscopy and Imaging Center (UMIC) (NWO-grant 40-00506-98-9021). The authors acknowledge Klaas Sjollema for assistance with TissueFaxs microscope.

Conflict of Interest

P.v.R. also is co-founder, scientific advisor, and share-holder of BiomACS BV, a biomedical oriented screening company. The authors declare no other competing interests.

Keywords

collagen, extracellular matrix, hierarchical topography, human mesenchymal stem cells, mechanotransduction, osteogenic differentiation

Received: March 3, 2020
Revised: April 2, 2020
Published online:

[1] C. H. Seo, H. Jeong, Y. Feng, K. Montagne, T. Ushida, Y. Suzuki, K. S. Furukawa, *Biomaterials* **2014**, *35*, 2245.
[2] M. P. Lutolf, P. M. Gilbert, H. M. Blau, *Nature* **2009**, *462*, 433.
[3] R. A. Marklein, J. A. Burdick, *Adv. Mater.* **2010**, *22*, 175.
[4] K. Yang, H. Jung, H. R. Lee, J. S. Lee, S. R. Kim, K. Y. Song, E. Cheong, J. Bang, S. G. Im, S. W. Cho, *ACS Nano* **2014**, *8*, 7809.
[5] Z. Chen, A. Bachhuka, S. Han, F. Wei, S. Lu, R. M. Visalakshan, K. Vasilev, Y. Xiao, *ACS Nano* **2017**, *11*, 4494.
[6] M. Lin, S. Mao, J. Wang, J. Xing, Y. Wang, K. Cai, Y. Luo, *Biomaterials* **2018**, *162*, 170.
[7] M. Wang, C. Cui, M. M. Ibrahim, B. Han, Q. Li, M. Pacifici, J. T. R. Lawrence, L. Han, L. H. Han, *Adv. Funct. Mater.* **2019**, *29*, 1808967.
[8] Y. Hou, L. Yu, W. Xie, L. C. Camacho, M. Zhang, Z. Chu, Q. Wei, R. Haag, *Nano Lett.* **2020**, *20*, 748.
[9] J. Baek, W.-B. Jung, Y. Cho, E. Lee, G.-T. Yun, S.-Y. Cho, H.-T. Jung, S. G. Im, *ACS Appl. Mater. Interfaces* **2019**, *11*, 17247.
[10] E. Ko, S. J. Yu, G. J. Pagan-Diaz, Z. Mahmassani, M. D. Boppart, S. G. Im, R. Bashir, H. Kong, *Adv. Sci.* **2019**, *6*, 1801521.
[11] J. Guerrero, S. Catros, S.-M. Derkaoui, C. Lalande, R. Siadous, R. Bareille, N. Thébaud, L. Bordenave, O. Chassande, C. Le Visage, D. Letourneur, J. Amédée, *Acta Biomater.* **2013**, *9*, 8200.
[12] Y. Aizawa, M. S. Shoichet, *Biomaterials* **2012**, *33*, 5198.
[13] B. Trappmann, J. E. Gautrot, J. T. Connelly, D. G. T. Strange, Y. Li, M. L. Oyen, M. A. Cohen Stuart, H. Boehm, B. Li, V. Vogel, J. P. Spatz, F. M. Watt, W. T. S. Huck, *Nat. Mater.* **2012**, *11*, 742.
[14] D. M. Le, K. Kulangara, A. F. Adler, K. W. Leong, V. S. Ashby, *Adv. Mater.* **2011**, *23*, 3278.
[15] A. J. Engler, S. Sen, H. L. Sweeney, D. E. Discher, *Cell* **2006**, *126*, 677.
[16] H. V Unadkat, M. Hulsman, K. Cornelissen, B. J. Papenburg, R. K. Truckenmüller, A. E. Carpenter, M. Wessling, G. F. Post, M. Uetz, M. J. T. Reinders, D. Stamatialis, C. A. van Blitterswijk, J. de Boer, *Proc. Natl. Acad. Sci. U. S. A.* **2011**, *108*, 16565.
[17] T. Dalgleish, J. M. G. Williams, A.-M. J. Golden, N. Perkins, L. F. Barrett, P. J. Barnard, C. A. Yeung, V. Murphy, R. Elward, K. Tchanturia, E. Watkins, *ACS Nano* **2013**, *136*, 23.
[18] K. K. B. Tan, J. Y. Tann, S. R. Sathe, S. H. Goh, D. Ma, E. L. K. Goh, E. K. F. Yim, *Biomaterials* **2015**, *43*, 32.
[19] M. J. Dalby, N. Gadegaard, R. O. C. Oreffo, *Nat. Mater.* **2014**, *13*, 558.
[20] E. H. Ahn, Y. Kim, Kshitiz, S. S. An , J. Afzal, S. Lee, M. Kwak, K. Y. Suh, D. H. Kim, A. Levchenko, *Biomaterials* **2014**, *35*, 2401.
[21] J. H. Kim, B. G. Park, S. K. Kim, D. H. Lee, G. G. Lee, D. H. Kim, B. O. Choi, K. B. Lee, J. H. Kim, *Acta Biomater.* **2019**, *95*, 337.
[22] S. L. Vega, V. Arvind, P. Mishra, J. Kohn, N. Sanjeeva Murthy, P. V. Moghe, *Acta Biomater.*. **2018**, *76*, 21.
[23] P. P. S. S. Abadi, J. C. Garbern, S. Behzadi, M. J. Hill, J. S. Tresback, T. Heydari, M. R. Ejtehadi, N. Ahmed, E. Copley, H. Aghaverdi, R. T. Lee, O. C. Farokhzad, M. Mahmoudi, *Adv. Funct. Mater.* **2018**, *28*, 1870128.
[24] Y.-J. Choi, S. J. Park, H.-G. Yi, H. Lee, D. S. Kim, D.-W. Cho, *J. Mater. Chem. B* **2018**, *6*, 5530.
[25] K. H. Song, S. J. Park, D. S. Kim, J. Doh, *Biomaterials* **2015**, *51*, 151.
[26] Q. Zhou, Z. Zhao, Z. Zhou, G. Zhang, R. C. Chiechi, P. van Rijn, *Adv. Mater. Interfaces* **2018**, *5*, 1800334.
[27] G. Abagnale, A. Sechi, M. Steger, Q. Zhou, C. C. Kuo, G. Aydin, C. Schalla, G. Müller-Newen, M. Zenke, I. G. Costa, P. van Rijn, A. Gillner, W. Wagner, *Stem Cell Rep.* **2017**, *9*, 654.
[28] Q. Zhou, O. C. Ocampo, C. F. Guimarães, P. T. Kühn, T. G. van Kooten, P. van Rijn, *ACS Appl. Mater. Interfaces* **2017**, *9*, 31433.
[29] Q. Zhou, P. Wünnemann, P. T. Kühn, J. de Vries, M. Helmin, A. Böker, T. G. van Kooten, P. van Rijn, *Adv. Mater. Interfaces* **2016**, *3*, 1600275.
[30] L. Lin, M. Liu, L. Chen, P. Chen, J. Ma, D. Han, L. Jiang, *Adv. Mater.* **2010**, *22*, 4826.
[31] J. J. Green, J. H. Elisseeff, *Nature* **2016**, *540*, 386.
[32] L. Rossetti, L. A. Kuntz, E. Kunold, J. Schock, K. W. Müller, H. Grabmayr, J. Stolberg-Stolberg, F. Pfeiffer, S. A. Sieber, R. Burgkart, A. R. Bausch, *Nat. Mater.* **2017**, *16*, 664.
[33] J. H. Wen, L. G. Vincent, A. Fuhrmann, Y. S. Choi, K. C. Hribar, H. Taylor-Weiner, S. Chen, A. J. Engler, *Nat. Mater.* **2014**, *13*, 979.
[34] Z. Yin, X. Chen, J. L. Chen, W. L. Shen, T. M. H. Nguyen, L. Gao, H. W. Ouyang, *Biomaterials* **2010**, *31*, 2163.
[35] P. Podsiadlo, A. K. Kaushik, E. M. Arruda, A. M. Waas, B. S. Shim, J. Xu, H. Nandivada, B. G. Pumplin, J. Lahann, A. Ramamoorthy, N. A. Kotov, *Science* **2007**, *318*, 80.
[36] M. Georgiou, S. C. J. Bunting, H. A. Davies, A. J. Loughlin, J. P. Golding, J. B. Phillips, *Biomaterials* **2013**, *34*, 7335.
[37] G. C. Engelmayr, M. Cheng, C. J. Bettinger, J. T. Borenstein, R. Langer, L. E. Freed, *Nat. Mater.* **2008**, *7*, 1003.
[38] Y. Li, Y. Xiao, C. Liu, *Chem. Rev.* **2017**, *117*, 4376.
[39] U. G. K. Wegst, H. Bai, E. Saiz, A. P. Tomsia, R. O. Ritchie, *Nat. Mater.* **2015**, *14*, 23.
[40] M. Foss, P. Kingshott, F. Besenbacher, J. L. Hansen, A. N. Larsen, J. Chevallier, D. C. Kraft, *ACS Nano* **2010**, *4*, 2874.
[41] J. Kim, W. G. Bae, H. W. Choung, K. T. Lim, H. Seonwoo, H. E. Jeong, K. Y. Suh, N. L. Jeon, P. H. Choung, J. H. Chung, *Biomaterials* **2014**, *35*, 9058.
[42] C. Y. Tay, H. Yu, M. Pal, W. S. Leong, N. S. Tan, K. W. Ng, D. T. Leong, L. P. Tan, *Exp. Cell Res.* **2010**, *316*, 1159.
[43] T. A. Petrie, J. E. Raynor, D. W. Dumbauld, T. T. Lee, S. Jagtap, K. L. Templeman, D. M. Collard, A. J. García, *Sci. Transl. Med.* **2010**, *2*, 45ra60.
[44] M. Prager-Khoutorsky, A. Lichtenstein, R. Krishnan, K. Rajendran, A. Mayo, Z. Kam, B. Geiger, A. D. Bershadsky, *Nat. Cell Biol.* **2011**, *13*, 1457.
[45] J. L. Charest, M. T. Eliason, A. J. García, W. P. King, *Biomaterials* **2006**, *27*, 2487.
[46] K. Zhang, H. Zheng, S. Liang, C. Gao, *Acta Biomater.*. **2016**, *37*, 131.
[47] Q. Zhou, P. T. Kühn, T. Huisman, E. Nieboer, C. van Zwol, T. G. van Kooten, P. van Rijn, *Sci. Rep.* **2015**, *5*, 16240.
[48] I. G. Kim, M. P. Hwang, P. Du, J. Ko, C. won Ha, S. H. Do, K. Park, *Biomaterials* **2015**, *50*, 75.
[49] J. Li, X. Mou, J. Qiu, S. Wang, D. Wang, D. Sun, W. Guo, D. Li, A. Kumar, X. Yang, A. Li, H. Liu, *Adv. Healthcare Mater.* **2015**, *4*, 998.
[50] A. A. Eid, K. A. Hussein, L. Niu, G. Li, I. Watanabe, M. Al-Shabrawey, D. H. Pashley, F. R. Tay, *Acta Biomater.*. **2014**, *10*, 3327.
[51] J. Qiu, J. Li, S. Wang, B. Ma, S. Zhang, W. Guo, X. Zhang, W. Tang, Y. Sang, H. Liu, *Small* **2016**, *12*, 1770.
[52] A. B. Faia-Torres, M. Charnley, T. Goren, S. Guimond-Lischer, M. Rottmar, K. Maniura-Weber, N. D. Spencer, R. L. Reis, M. Textor, N. M. Neves, *Acta Biomater.* **2015**, *28*, 64.
[53] S. Fusco, V. Panzetta, V. Embrione, P. A. Netti, *Acta Biomater.* **2015**, *23*, 63.
[54] I. Lauria, M. Kramer, T. Schröder, S. Kant, A. Hausmann, F. Böke, R. Leube, R. Telle, H. Fischer, *Acta Biomater.* **2016**, *44*, 85.

[55] C. Zhou, D. Zhang, J. Zou, X. Li, S. Zou, J. Xie, *ACS Appl. Mater. Interfaces* **2019**, *11*, 26448.
[56] S. Dupont, L. Morsut, M. Aragona, E. Enzo, S. Giulitti, M. Cordenonsi, F. Zanconato, J. Le Digabel, M. Forcato, S. Bicciato, N. Elvassore, S. Piccolo, *Nature* **2011**, *474*, 179.
[57] S. Musah, P. J. Wrighton, Y. Zaltsman, X. Zhong, S. Zorn, M. B. Parlato, C. Hsiao, S. P. Palecek, Q. Chang, W. L. Murphy, L. L. Kiessling, *Proc. Natl. Acad. Sci. U. S. A.* **2014**, *111*, 13805.
[58] L. Azzolin, T. Panciera, S. Soligo, E. Enzo, S. Bicciato, S. Dupont, S. Bresolin, C. Frasson, G. Basso, V. Guzzardo, A. Fassina, M. Cordenonsi, S. Piccolo, *Cell* **2014**, *158*, 157.
[59] S. R. Caliari, S. L. Vega, M. Kwon, E. M. Soulas, J. A. Burdick, *Biomaterials* **2016**, *103*, 314.
[60] S. Lee, A. E. Stanton, X. Tong, F. Yang, *Biomaterials* **2019**, *202*, 26.
[61] M. Bao, J. Xie, A. Piruska, W. T. S. Huck, *Nat. Commun.* **2017**, *8*, 1.
[62] C. Cha, W. B. Liechty, A. Khademhosseini, N. A. Peppas, *ACS Nano* **2012**, *6*, 9353.
[63] R. K. Das, O. F. Zouani, *Biomaterials* **2014**, *35*, 5278.
[64] G. Abagnale, M. Steger, V. H. Nguyen, N. Hersch, A. Sechi, S. Joussen, B. Denecke, R. Merkel, B. Hoffmann, A. Dreser, U. Schnakenberg, A. Gillner, W. Wagner, *Biomaterials* **2015**, *61*, 316.
[65] S. H. Oh, D. B. An, T. H. Kim, J. H. Lee, *Acta Biomater.* **2016**, *35*, 23.
[66] H. Yuan, Y. Zhou, M.-S. Lee, Y. Zhang, W.-J. Li, *Acta Biomater.* **2016**, *42*, 247.
[67] B. K. K. Teo, S. T. Wong, C. K. Lim, T. Y. S. Kung, C. H. Yap, Y. Ramagopal, L. H. Romer, E. K. F. Yim, *ACS Nano* **2013**, *7*, 4785.
[68] W. Chen, L. G. Villa-Diaz, Y. Sun, S. Weng, J. K. Kim, R. H. W. Lam, L. Han, R. Fan, P. H. Krebsbach, J. Fu, *ACS Nano* **2012**, *6*, 4094.
[69] X. Yao, R. Peng, J. Ding, *Biomaterials* **2013**, *34*, 930.
[70] C. H. Seo, K. Furukawa, K. Montagne, H. Jeong, T. Ushida, *Biomaterials* **2011**, *32*, 9568.